

Electronic supplementary information

Concentration dependent tautomerism in green $[\text{Cu}(\text{HL}^1)(\text{L}^2)]$ and brown $[\text{Cu}(\text{L}^1)(\text{HL}^2)]$ with $\text{H}_2\text{L}^1 = (\text{E})\text{-N}'\text{-}(2\text{-hydroxy-3-methoxybenzylidene})\text{benzoylhydrazone}$ and $\text{HL}^2 = \text{pyridine-4-carboxylic (isonicotinic) acid}$

Hassan Hosseini Monfared^{a*}, Morteza Vahedpour^a, Mahdi Mahdavi Yeganeh^a, Massomeh Ghorbanloo^a, Peter Mayer^b and Christoph Janiak^{c,d}

^a Department of Chemistry, Faculty of Sciences, Zanjan University 45195-313, Zanjan, I.R. Iran.

Email: monfared@znu.ac.ir

^b Fakultät für Chemie und Pharmazie, Ludwig-Maximilians-Universität, München, Butenandtstr. 5-13, Haus D, D-81377 München, Germany

^c Institut für Anorganische und Analytische Chemie, Universität Freiburg, Albertstr. 21, 79104 Freiburg, Germany.

^d New address: Institut für Anorganische Chemie und Strukturchemie, Universität Düsseldorf, Universitätsstr. 1, 40225 Düsseldorf, Germany. Email: janiak@uni-duesseldorf.de

Peter Mayer: pemay@cup.uni-muenchen.de

Morteza Vahedpour: vahed@znu.ac.ir

Mahdi Mahdavi Yeganeha: yeganeha@znu.ac.ir

Massomeh Ghorbanloo: m_ghorbanloo@yahoo.com

Content:	page
Appendix S1: Further details on metal-nucleobase tautomers, $[\text{Os}(\eta^2\text{-H}_2)(\text{CO})(\text{quS})(\text{PPh}_3)_2]^+$ and $[\text{Os}(\text{H})(\text{CO})(\text{quSH})(\text{PPh}_3)_2]^+$ tautomers and tautomerism in Mg^{2+} sensor	2
Fig. S1 Infrared spectrum of green- $[\text{Cu}(\text{HL}^1)(\text{L}^2)]\cdot\text{H}_2\text{O}\cdot\text{C}_2\text{H}_5\text{OH}$ (1) as KBr pellet.	3
Fig. S2 Infrared spectrum of brown- $[\text{Cu}(\text{L}^1)(\text{HL}^2)]$ (2) as KBr pellet.	3
Table S1 Distances (d/Å) and angles (°) for the π-stacking interactions in 1 and 2 .	4
Fig. S3 UV/VIS spectra of green- $[\text{Cu}(\text{HL}^1)(\text{L}^2)]\cdot\text{H}_2\text{O}\cdot\text{C}_2\text{H}_5\text{OH}$ (1) and brown- $[\text{Cu}(\text{L}^1)(\text{HL}^2)]$ (2)	5
Fig. S4 Frontier molecular orbitals of green- 1 .	7
Fig. S5 Frontier molecular orbitals of brown- 2 .	8
Fig. S6-S8 Crystal pictures of 1 and 2	9

Appendix S1: Further details also on metal-nucleobase tautomers, $[\text{Os}(\eta^2\text{-H}_2)(\text{CO})(\text{quS})(\text{PPh}_3)_2]^+$ and $[\text{Os}(\text{H})(\text{CO})(\text{quSH})(\text{PPh}_3)_2]^+$ tautomers and tautomerism in Mg^{2+} sensor

A mixed nucleobase complex of Hg(II) has been prepared which contains the rare imino tautomer form of the model nucleobase 9-methyladenine.¹ Stabilization of the 7*H*-adenine tautomer in the solid-state by the interaction of the purine nucleobase with metal-oxalato frameworks has been reported.² In the coordination chemistry of uracil and thymine (5-methyluracil) such factors as the metal, reaction time, pH, packing factors, noncovalent interactions and solvent may exert more influence on tautomer selection.³ The iminooxo tautomer of cytosine coordinated to Pt(II) with metal and nucleobase in *syn* and *anti* orientations⁴ was stabilized. Ru(III) coordination to the exocyclic nitrogen of 9-methyladenine and stabilisation of the rare imine tautomer by intramolecular hydrogen bonding has been reported.⁵ The relative stability of 1-methyluracil through coordination of these tautomers to Pt^{II} complexes has been studied computationally.⁶ The rare iminol tautomer of 1-methylthymine through metal coordination at N(3) was reported.⁷ A way is presented⁸ according to which the geometry of rare nucleobase tautomers is estimated by (i) preparing metal complexes of the rare tautomers, (ii) determining the crystal structure of the metal complex as accurately as possible, and (iii) "subtracting" the effect of the metal on the ligand geometry. Influence of the anion on the non-covalent stabilization of 7*H*-adenine tautomer in metal–nucleobase interactions in magnesium(II) and manganese(II) complexes with adenine has been studied.⁹ A simple fluorescent sensor has been developed¹⁰ for the ratiometric recognition of Mg^{2+} in semi-aqueous solution at pH 7.0. The sensor, a Schiff base, undergoes Excited State Intramolecular Proton Transfer (ESIPT) to generate a keto tautomer with proficient Mg^{2+} binding capability. The sensor displays good selectivity over other metal ions including alkali/alkali earth ions and can measure Mg^{2+} ion concentration between 2.0 and 30.0 μM . The binding stoichiometry was established as 2:1 (host:guest) with an association constant (K_{21}) of $(1.4 \pm 0.1) \times 10^4 \text{ M}^{-2}$. The sensor could potentially be used to detect conditions such as hypermagnesaemia. The mixture of two isomers of the complex $\text{Os}(\text{H})(\text{CO})(\text{quS})(\text{PPh}_3)_2$ reacts with $\text{HBF}_4 \cdot \text{Et}_2\text{O}$ at -80°C to form the complexes $[\text{Os}(\eta^2\text{-H}_2)(\text{CO})(\text{quS})(\text{PPh}_3)_2]^+$ with dihydrogen *trans* to sulfur or nitrogen along with tautomeric thiol complexes $[\text{Os}(\text{H})(\text{CO})(\text{quSH})(\text{PPh}_3)_2]^+$ (quS = quinolin-8-thiolate); the tautomeric equilibria shift with temperature.¹¹ The influence of Cd^{2+} on nucleobases and base pairing has been studied systematically using high-level DFT method with the purpose to investigate the interaction between Cd^{2+} and nucleobases systems via the first-principle DFT method to gain insights into DNA mutation.¹²

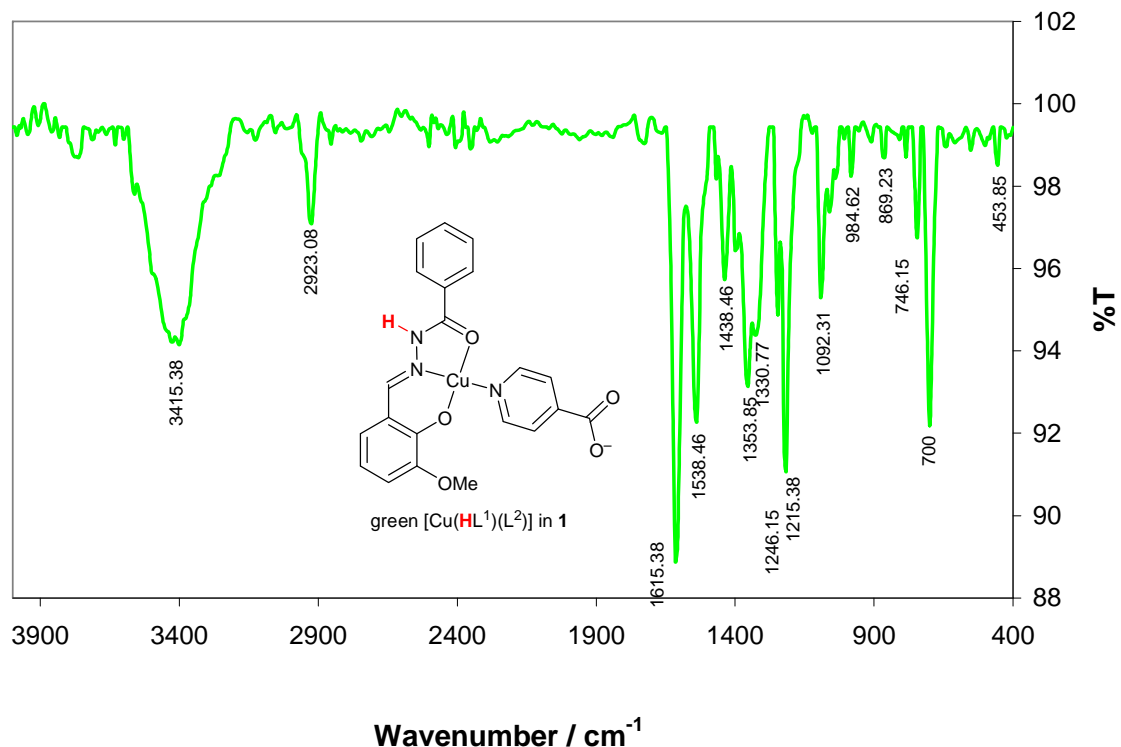


Fig. S1 Infrared spectrum of green- $[\text{Cu}(\text{HL}^1)(\text{L}^2)] \cdot \text{H}_2\text{O} \cdot \text{C}_2\text{H}_5\text{OH}$ (**1**) as KBr pellet.

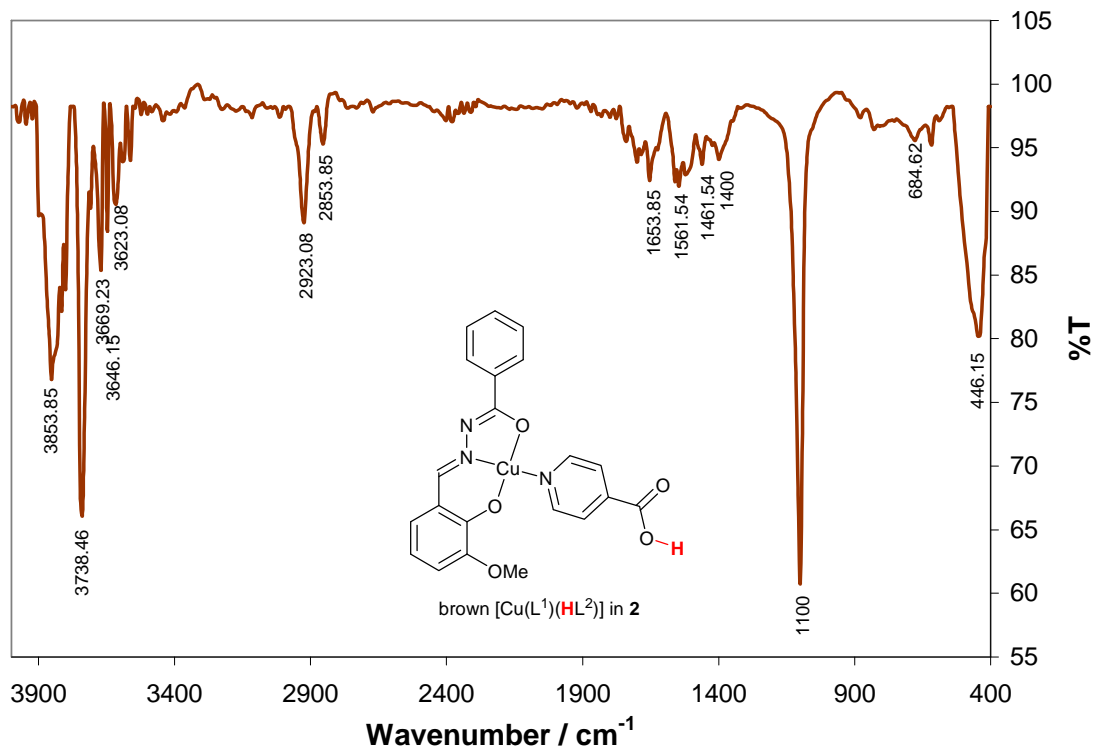


Fig. S2 Infrared spectrum of brown- $[\text{Cu}(\text{L}^1)(\text{HL}^2)]$ (**2**) as KBr pellet.

Table S1 Distances (d/Å) and angles (°) for the π -stacking interactions in **1** and **2**.^a

compound 1 (see Fig. 5)		[Ct(I)···Ct(J)] ^c	α ^d	β ^e	γ ^f	d[Ct(I)···P(J)] ^g	d[Ct(J)···P(I)] ^h
ring(I)···ring(J)	symm ^b	3.659(2)	14.9	9.1	17.9	3.482(1)	3.614(1)
ring 3···ring 3'	[4554]	3.671(2)	10.8(1)	31.1	21.8	3.408(1)	3.142(1)
ring 4···ring 1	[3757]	3.448(2)	3.1(1)	17.5	17.0	3.298(1)	3.288(1)
ring 4···ring 2	[3757]	3.975(2)	3.1(1)	26.2	28.8	3.484(1)	3.566(1)
ring 4···ring 5	[3756]	3.642(2)	1.6(1)	12.0	13.3	3.544(1)	3.563(1)

ring 1: Cu-O1-N1-N2-C1 (five-membered chelate); ring 2, 2': Cu-O2-N2-C8-C9-C10 (six-membered chelate);
 ring 3, 3': N3-C16-C17-C18-C19-C20 (pyridyl); ring 4: C2-C3-C4-C5-C6-C7 (benzoyl);
 ring 5: C9-C10-C11-C12-C13-C14 (salicyl).

^b symmetry transformations: [3756] = 2-x, -y, 1-z; [3757] = 2-x, -y, 2-z; [4554] = x, 0.5-y, -0.5+z.

compound **2** (see Fig. 7)

ring(I)···ring(J)	symm ⁱ	[Ct(I)···Ct(J)] ^c	α ^d	β ^e	γ ^f	d[Ct(I)···P(J)] ^g	d[Ct(J)···P(I)] ^h
ring 2···ring 1	[1455]	3.555(2)	5.7(2)	16.0	10.5	3.496(2)	3.419(2)
ring 5···ring 1	[1455]	3.819(2)	4.3(2)	26.7	30.5	3.291(2)	3.411(2)
ring 5···ring 2'	[1455]	3.576(2)	1.4(2)	19.4	20.1	3.358(2)	3.372(2)

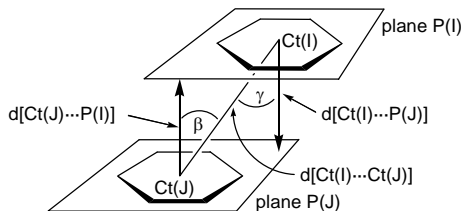
ring 1: Cu-O1-N1-N2-C1;

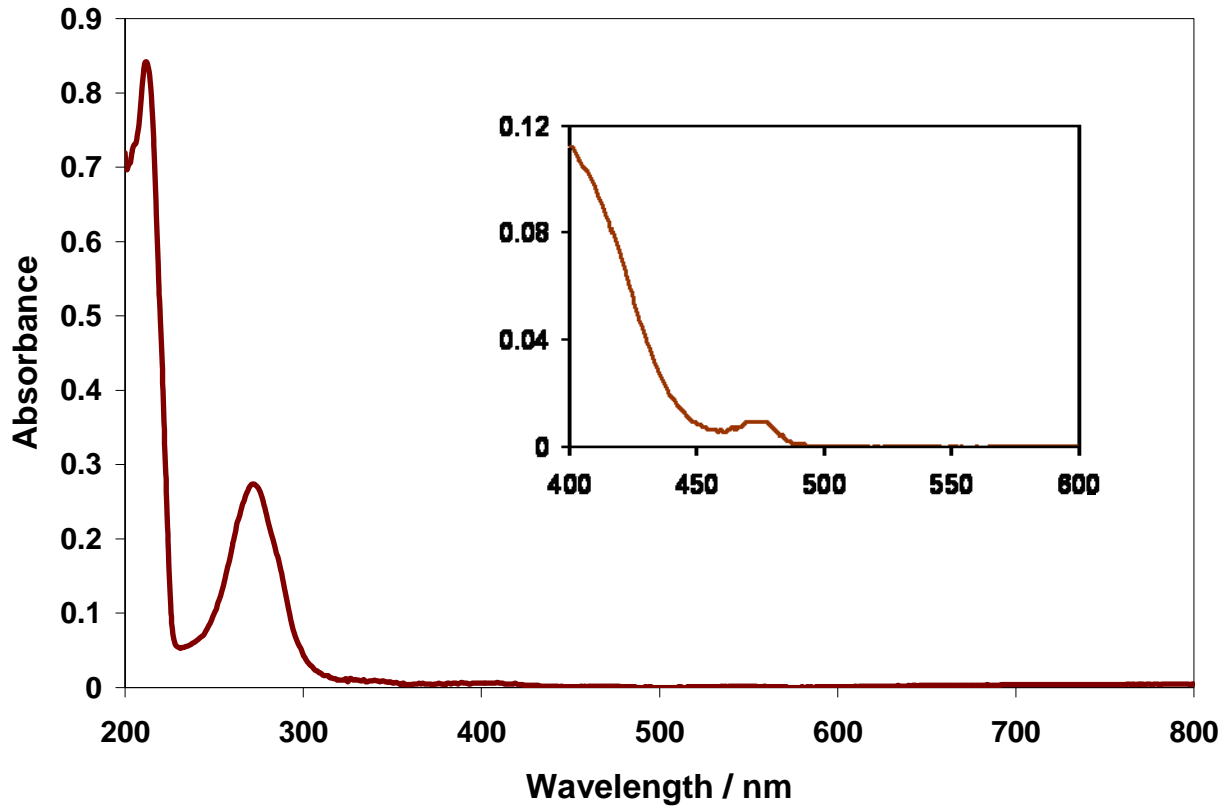
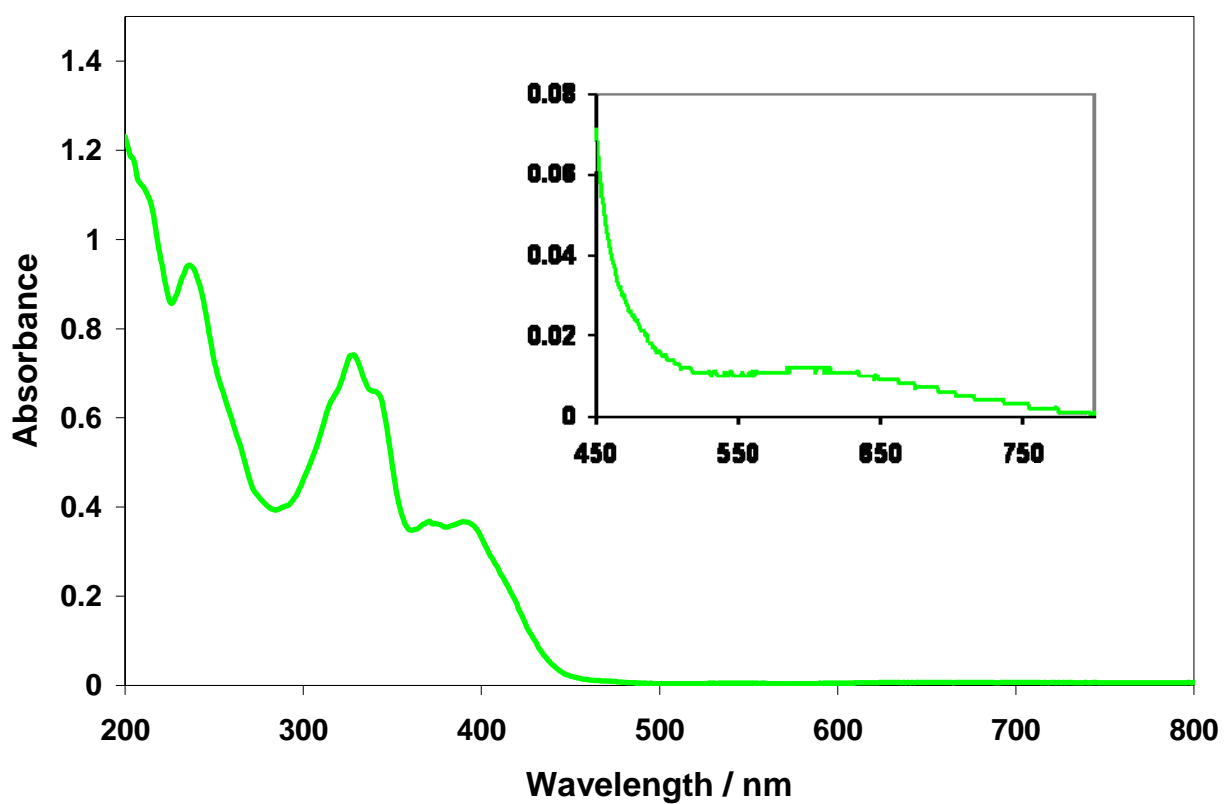
ⁱ symmetry transformations [1455] = -1+x, y, z

ring 2, 2': Cu-O2-N2-C8-C9-C10;

ring 5: C9-C10-C11-C12-C13-C14 (salicyl).

^a For a graphical depiction of distances and angles in the assessment of the π -contacts, see Scheme S1. – ^c Centroid-centroid distance. – ^d Dihedral angle between the ring planes. – ^e Angle between the centroid vector Ct(I)···Ct(J) and the normal to the plane I ("slip angle"). – ^f Angle between the centroid vector Ct(I)···Ct(J) and the normal to the plane J. – ^g Perpendicular distance of Ct(I) on ring plane J. – ^h Perpendicular distance of Ct(J) on ring plane I.

**Scheme S1** Graphical presentation of the parameters used in Table 3 for the description of π -stacking.



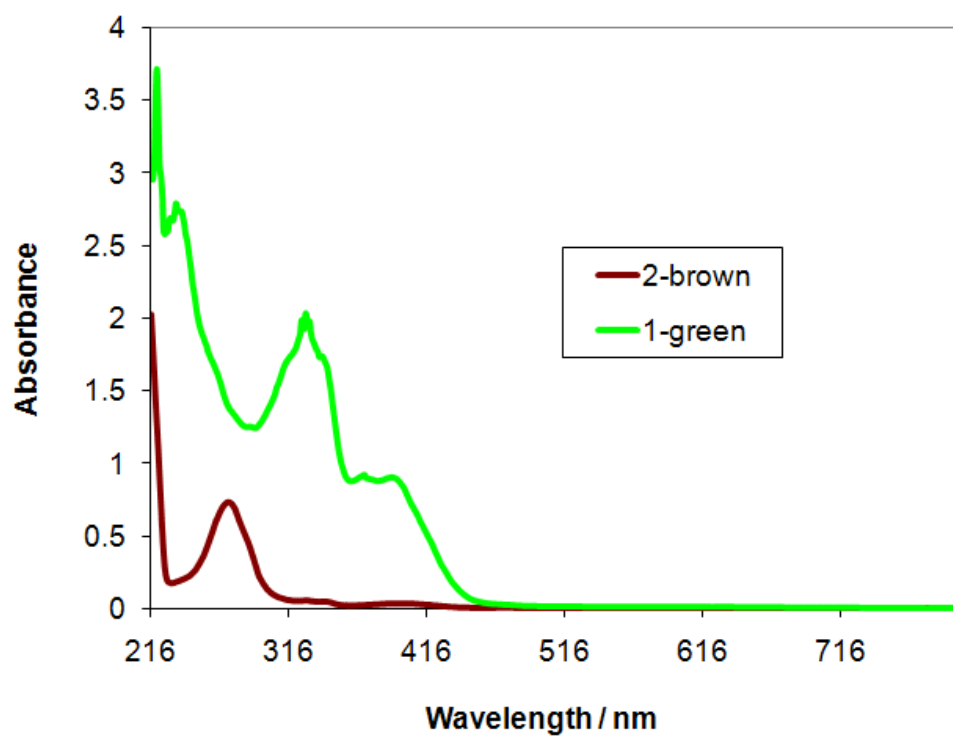


Fig. S3 UV/VIS spectra of green-[Cu(HL¹)(L²)]·H₂O·C₂H₅OH (**1**) and brown-[Cu(L¹)(HL²)] (**2**) in CH₃CN

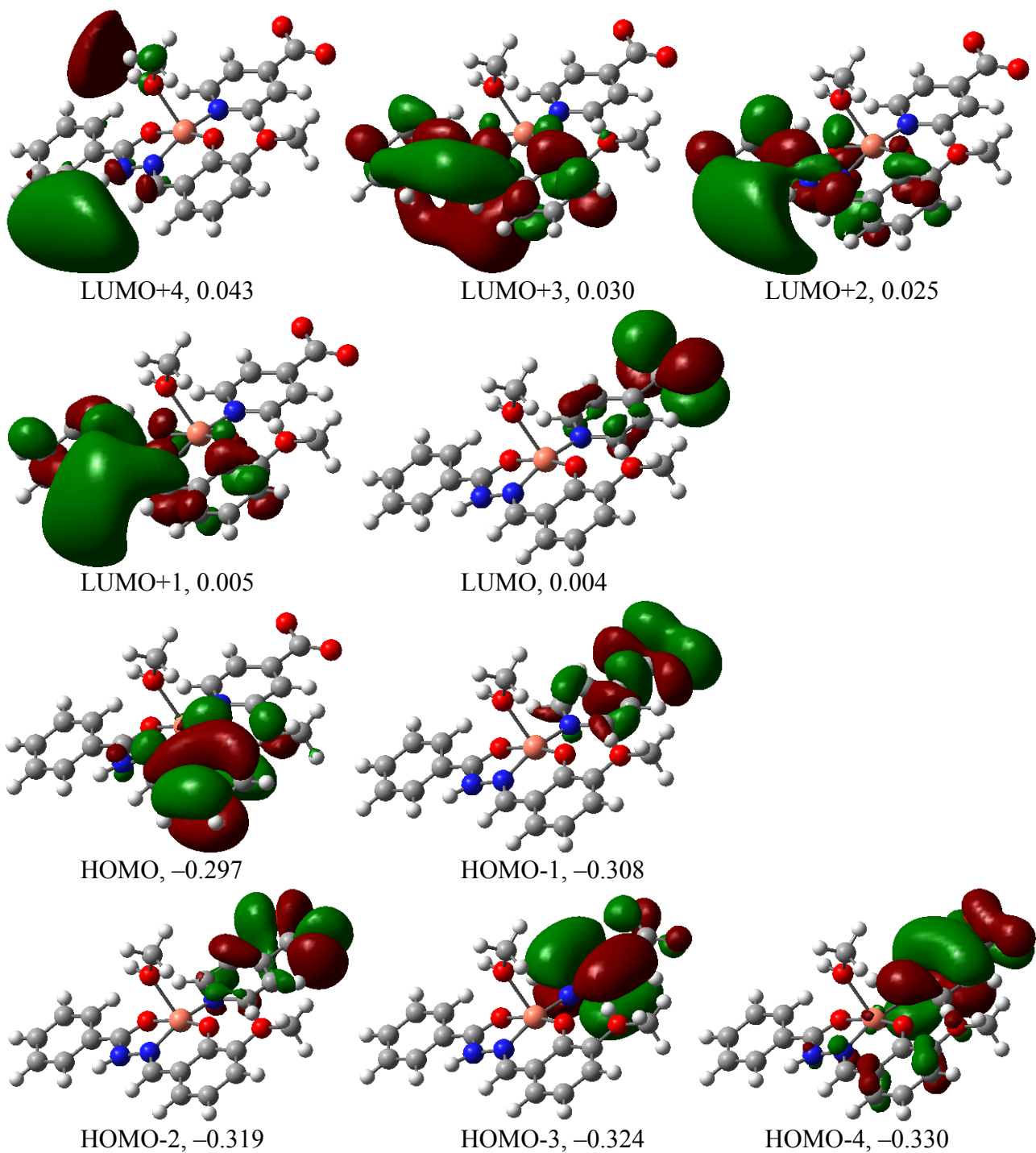


Fig. S4 Frontier molecular orbitals of green-1, with the energy eigenvalues in eV.

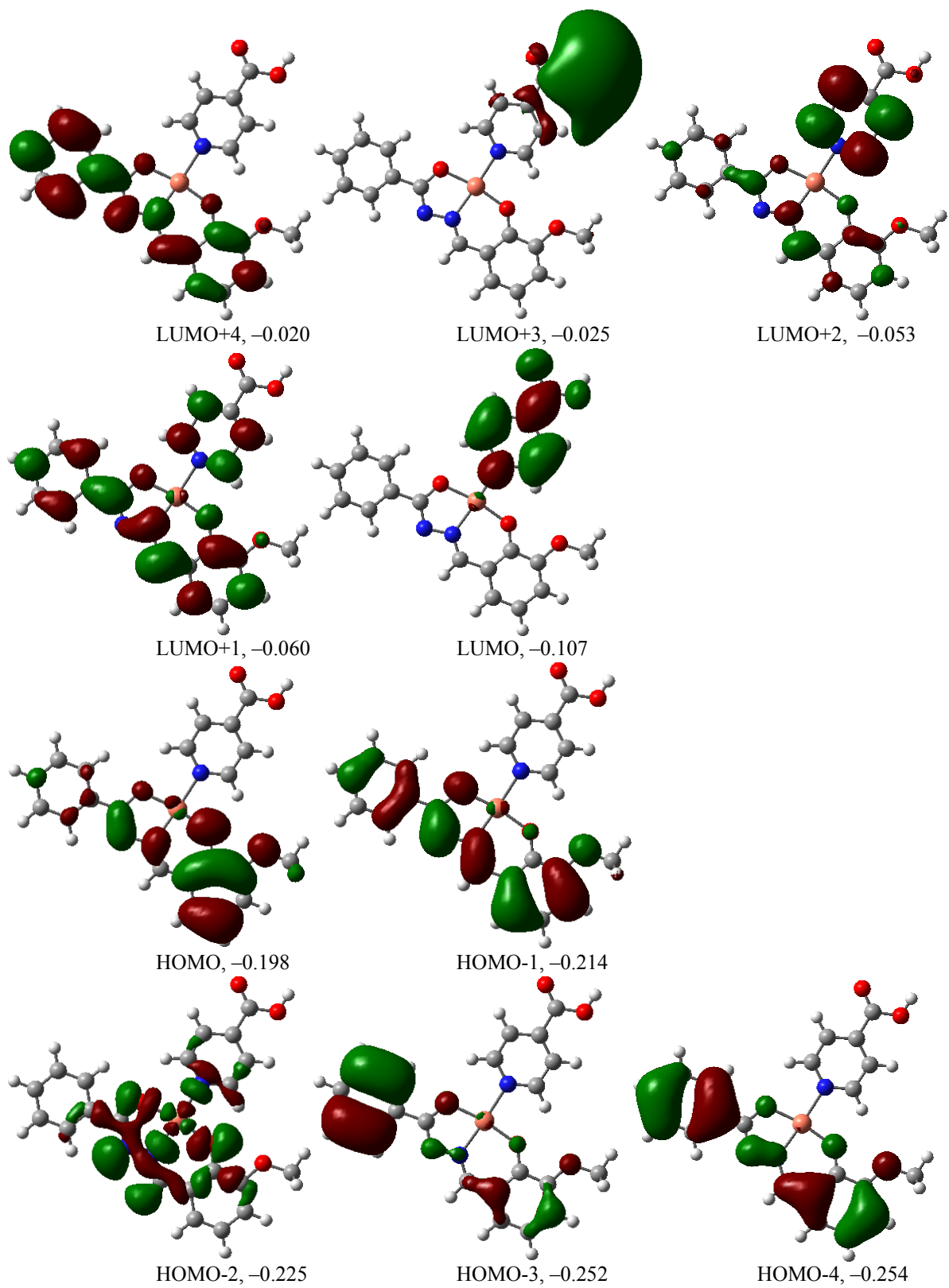


Fig. S5 Frontier molecular orbitals of brown-2, with the energy eigenvalues in eV.

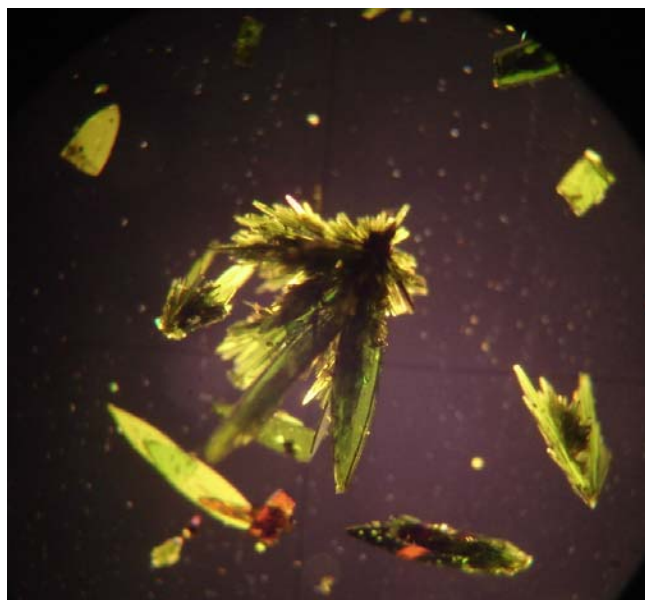


Fig. S6 Crystals from experiment no. 1 showing green-[Cu(HL¹)(L²)]·H₂O·C₂H₅OH (**1**) as major and brown-[Cu(L¹)(HL²)] (**2**) as minor component before the manual separation.

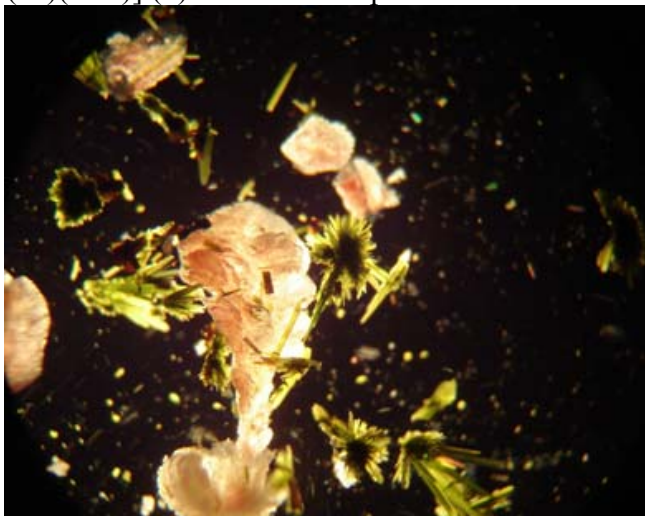


Fig. S7 Crystals from experiment no. 2 showing green-[Cu(HL¹)(L²)]·H₂O·C₂H₅OH (**1**) and brown-[Cu(L¹)(HL²)] (**2**) as about equal components before the manual separation.

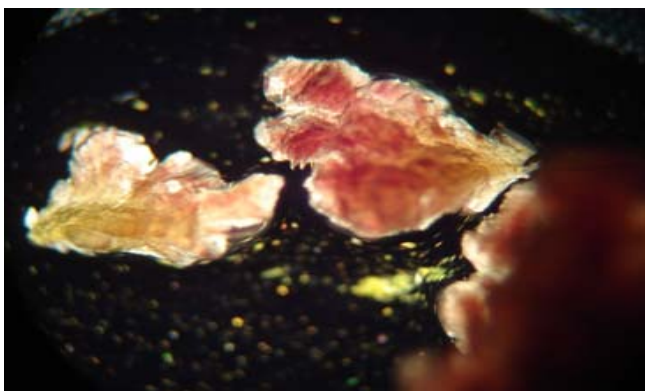


Fig. S8 Crystals from experiment no. 3 showing green-[Cu(HL¹)(L²)]·H₂O·C₂H₅OH (**1**) as very minor and brown-[Cu(L¹)(HL²)] (**2**) as major component before the manual separation.

-
- 2 J. P. García-Terán, O. Castillo, A. Luque, U. García-Couceiro, G. Beobide and P. Román, *Dalton Trans.*, 2006, 902–911.
- 3 (a) I. Mutikainen and P. Lumme, *Acta Crystallogr., Sect. B* 1980, **36**, 2237-2240; (b) R. Pfab, P. Jandík and B. Lippert, *Inorg. Chem. Acta*, 1982, **66**, 193- 204; (c) I. Escorihuela, L. R. Falvello, M. Tomás and E. P. Urriolabeitia, *Cryst. Growth Des.*, 2004, **4**, 655-657.
- 4 F. Pichierri, D. Holthenrich, E. Zangrando, B. Lippert and L. Randaccio, *J. Biol. Inorg. Chem.*, 1996, **1**, 439-445.
- 5 A. H. Velders, B. Geest, H. Kooijman, A. L. Spek, J. G. Haasnoot and J. Reedijk, *Eur. J. Inorg. Chem.*, 2001, 369-372.
- 6 T. Wijst, C. F. Guerra, M. Swart, F. M. Bickelhaupt and B. Lippert, *Chem. Eur. J.*, 2009, **15**, 209-218.
- 7 B. Lippert, *Inorg. Chim. Acta*, 1981, **55**, 5-14
- 8 B. Lippert, H. Schöllhorn and U. Thewalt, *J. Am. Chem. Soc.*, 1986, **108**, 6616-6621.
- 9 T. F. Mastropietro, D. Armentano, N. Marino and G. D. Munno, *Polyhedron*, 2007, **26**, 4945-4954.
- 10 N. Singh, N. Kaur, R. C. Mulrooney and J. F. Callan, *Tetrahedron Lett.*, 2008, **49**, 6690-6692
- 11 M. Schlaf and R. H. Morris, *J. Chem. Soc., Chem. Commun.*, 1995, 625.
- 12 Y. Wu, R. Sa, Q. Li, Y. Wei and K. Wu, *Chem. Phys. Lett.*, 2009, **467**, 387-392.